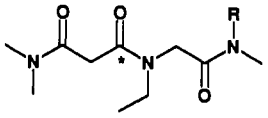

1, R = H	1641	1614	cm^{-1}
4, R = CH_3	1650	1606	cm^{-1}
Δ	+9	-8	

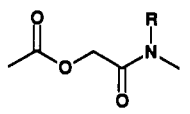

5, R = H	1757	cm^{-1}
6, R = CH_3	1751	cm^{-1}
Δ	-6	

a methyl group in **4** results in the amide I band of the nine-membered-ring acceptor moving 9 cm^{-1} to higher wavenumber, which is consistent with the loss of a hydrogen bond accepting role for this carbonyl. The labeled amide group, on the other hand, moves 8 cm^{-1} to *lower* wavenumber in **4**. The direction of this shift is not consistent with a hydrogen bond accepting role for the labeled carbonyl in **1**. The −8-cm^{-1} shift is apparently a general result of the covalently remote methylation, as indicated by the ester C=O stretch data for **5** and **6**. (The lone NH stretch of 1 mM **5** in CH_2Cl_2 occurs at 3454 cm^{-1}, demonstrating that there is no intramolecular hydrogen bonding in this amide–ester under these conditions.) These IR data indicate that the internal hydrogen bond of **1** is not bifurcated in solution.[5]

Invalidation of the bifurcation hypothesis suggested that the trans double bond of diamide **3** is not an adequate model for the purely structural role played by the central amide in stabilizing folding pattern **1a**. The central rotationally restricted C—N bond of **1** has four non-hydrogen substituents, while the analogous C=C bond of **3** has only two non-hydrogen substituents. We prepared diamide **7**,[4] containing a tetrasubstituted C=C bond, in order to determine whether additional sterically demanding substituents around the central rotationally restricted linkage could affect the stability of the internally hydrogen bonded state.[6] The IR N–H stretch signature of **7** in CH_3CN (Figure 1d) reveals this molecule to be predominantly internally hydrogen bonded, in contrast to diamide **3**, but similar to triamide **1**.[7]

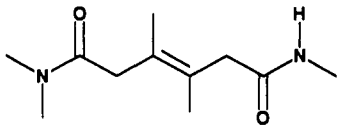

7

One might now ask whether the intramolecular hydrogen bond itself imparts any stability to folding pattern **1a**.[8] We addressed this question by examining **8**,[4] in which the terminal dimethyl amide moiety, a strong hydrogen-bond acceptor, is replaced by a methyl ester, a much weaker acceptor.[9] The N–H stretch region for **8** (1 mM in CH_2Cl_2) shows two bands, at 3392 and 3445 cm^{-1}. The former arises from N–H hydrogen bonded to an ester carbonyl; the latter arises from a non-hydrogen-bonded N–H. The 3392-cm^{-1} band is the larger of the two, indicating that **8** experiences substantial nine-membered-ring hydrogen bonding under these conditions. However, the non-hydrogen-bonded N–H stretch band of **8** is significantly larger than the analogous band for **1** under identical conditions, which demonstrates that the stability of folding pattern **1a** does indeed depend in part on the strength of the intramolecular hydrogen bond.

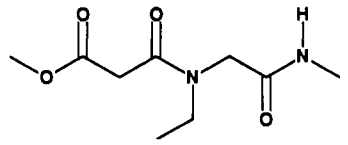

8

We have shown that at least three distinct factors contribute to the stability of folding pattern **1a**. The strong intramolecular hydrogen bond, the central nonrotating bond in the segment linking the hydrogen-bond donor and acceptor, and additional, more subtle torsional restrictions about sp^3–sp^2 bonds in the linking segment all appear to play important roles in stabilizing the conformation containing a nine-membered hydrogen-bonded ring. We are unaware of previous studies in which the network of internal noncovalent forces stabilizing the folding pattern of a natural or unnatural peptide has been elucidated at this level of detail. Parallel experiments with larger peptides are in progress.

Acknowledgment. We are grateful for partial support from the National Science Foundation (CHE 9104488) and the Searle Scholars Program. S.H.G. thanks the American Cancer Society for a Junior Faculty Research Award, and G.-B.L. thanks BP America for a fellowship.

(5) A referee has suggested that the geometry of the hydrogen bond involving the central amide carbonyl in hypothetical conformation **1b** could be so distorted (proton far out of the plane of the acceptor carbonyl) that the usual amide I shift to lower wavenumber would not be observed. We do not known of any published data that bear upon this suggestion.

(6) For a recent review covering the literature on torsional barriers associated with variously substituted sp^2–sp^3 bonds, see: Berg, U.; Sandström, J. *Adv. Phys. Org. Chem.* **1989**, *25*, 1.

(7) Crystallographic analysis of diamide **7** reveals that the nine-membered-ring hydrogen bond is retained in the solid state (Liang, G.-B.; Desper, J. M., unpublished results).

(8) Computational results led Synder to conclude that two observed intramolecular hydrogen bonds in the cyclic depsipeptide roseotoxin B are not a primary source of conformational rigidity; rather, these hydrogen bonds appear to be largely a consequence of other rigidifying factors. Snyder, J. P. *J. Am. Chem. Soc.* **1984**, *106*, 2393.

(9) (a) Arnett, E. M.; Mitchell, E. J.; Murty, T. S. S. R. *J. Am. Chem. Soc.* **1974**, *96*, 3875. (b) Spencer, J. N.; Garrett, R. C.; Moyer, F. J.; Merkle, J. E.; Powell, C. R.; Tran, M. T.; Berger, S. K. *Can. J. Chem.* **1980**, *58*, 1372.

Reactions and Rate Constants between Hydrated Electrons and the Monomer and Dimer of 2-Methyl-2-nitrosopropane Determined by the Pulse Radiolysis Method

Mikinori Kuwabara,*,† Wakako Hiraoka,† Sadashi Sawamura,‡ and Meiseki Katayama‡

Department of Radiation Biology, Faculty of Veterinary Medicine, and Department of Atomic Science and Nuclear Engineering, Faculty of Engineering Hokkaido University, Sapporo 060, Japan

Received July 19, 1990
Revised Manuscript Received March 11, 1991

The spin trapping method[1] is now widely applied in chemistry, biology, and medicine regarding free radicals. In particular, free radicals induced in biologically significant molecules by ionizing radiation have been identified by this method to elucidate the primary processes in radiation biology.[2-9] In spin trapping studies, 2-methyl-2-nitrosopropane (MNP) has been frequently employed as the spin trap because this is suitable for identification of the radical structures. Ionizing radiation produces hydroxyl radicals (OH$^\bullet$), hydrated electrons (e_{aq}^-), and atomic hydrogen (H$^\bullet$) in an aqueous system. These radicals react not only with biological molecules but also with the spin trap. This means that MNP traps free radicals from biological molecules to form spin adducts and free radicals from MNP itself to induce byproducts. Sargent and

† Department of Radiation Biology, Faculty of Veterinary Medicine.
‡ Department of Atomic Science and Nuclear Engineering, Faculty of Engineering.

(1) Janzen, E. G. *Acc. Chem. Res.* **1971**, *4*, 31–40.
(2) Kuwabara, M.; Inanami, O.; Endoh, D.; Sato, F. *Biochemistry* **1989**, *28*, 9625–9632.
(3) Riesz, P.; Rustgi, S. *Radiat. Phys. Chem.* **1979**, *13*, 21–40.
(4) Riesz, P.; Rosenthal, I. *Can. J. Chem.* **1982**, *60*, 1474–1479.
(5) Rosenthal, I.; Riesz, P. *Radiat. Phys. Chem.* **1987**, *30*, 381–387.
(6) Kuwabara, M.; Inanami, O.; Sato, F. *Int. J. Radiat. Biol.* **1986**, *49*, 829–844.
(7) Inanami, O.; Kuwabara, M.; Hayashi, M.; Yoshii, G.; Syuto, B.; Sato, F. *Int. J. Radiat. Biol.* **1986**, *49*, 47–56.
(8) Inanami, O.; Kuwabara, M.; Sato, F. *Free Radical Res. Commun.* **1988**, *5*, 43–49.
(9) Feix, J. B.; Kalyanaraman, B. *Biochim. Biophys. Acta* **1989**, *992*, 230–235.

0002-7863/91/1513-3995$02.50/0

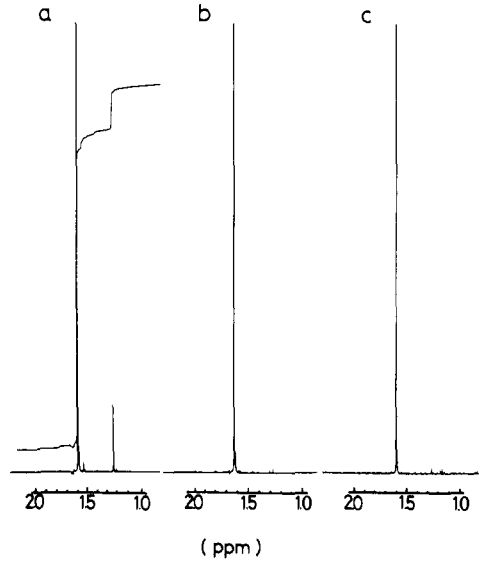

Figure 1. ^1H NMR spectra of (a) the solution in which MNP powder was dissolved and stirred for 12 h under anaerobic conditions, (b) the solution immediately after MNP powder was dissolved, and (c) the solution immediately after solution a was again bubbled with Ar gas for 30 min.

Gardy reported the ESR spectra of MNP–OH and MNP–H adducts,[10] but it is well-known that these spectra disappeared rapidly due to the instability of the adducts and were, therefore, not useful for the estimation of byproducts. To estimate exactly the relative concentrations of the spin adducts and the byproducts, it is necessary to know the rate constants between water radicals and MNP. The rate constants for the reaction between MNP and OH• and H• have already been reported to be 5×10^9 [mol^{-1} s^{-1}] and 1.9×10^9 [mol^{-1} s^{-1}], respectively, by Greenstock,[11] but detailed information concerning the measurements was not provided. Furthermore, the rate constant for the reaction between e_{aq}^- and MNP remains unreported. In the present study, we carried out pulse radiolysis experiments to determine the rate constant for the reaction between e_{aq}^- and MNP.

MNP is present in both dimer and monomer forms in aqueous solutions. Although it has been reported that the relative intensities of dimer and monomer measured by NMR spectrometry change with the time after MNP powder is dissolved, their definite concentrations have not been given.[3] For pulse radiolysis experiments the absolute concentrations of the dimer and monomer forms are required. Dissolution of 1 mg of MNP in 1 mL of aqueous solution is theoretically calculated to give concentrations of 11.5 mmol for monomer and 5.75 mmol for dimer, but MNP tends to decompose to other products,[12] and the monomer form becomes volatile. Thus, a reliable method to determine molar concentrations is to use the molar absorption coefficient ϵ (=8000) of the dimer at 295 nm.[12] The molar concentrations of the monomer are then calculated from [dimer]/[monomer] ratios determined by NMR measurements. Figure 1 shows ^1H NMR spectra of the MNP dimer and monomer. The NMR measurements were performed by using a Bruker MSL-400 spectrometer. The peaks at the chemical shift with δ 1.28 and 1.59 ppm correspond to the dimer and monomer, respectively. Figure 1a shows the NMR spectrum obtained after 2.45 mg of MNP powder was added to 1 mL of D_2O, followed by bubbling for 30 min with Ar gas and stirring for 12 h in the dark. Figure 1b shows the NMR spectrum obtained immediately after the powder was dissolved and Ar-bubbled for 30 min. The ratio of [dimer]/[monomer] was 44. Figure 2 shows plots of the concentration vs time after Ar-bubbling. This figure shows that while the decrease in the concentration of the dimer was relatively rapid during stirring, the

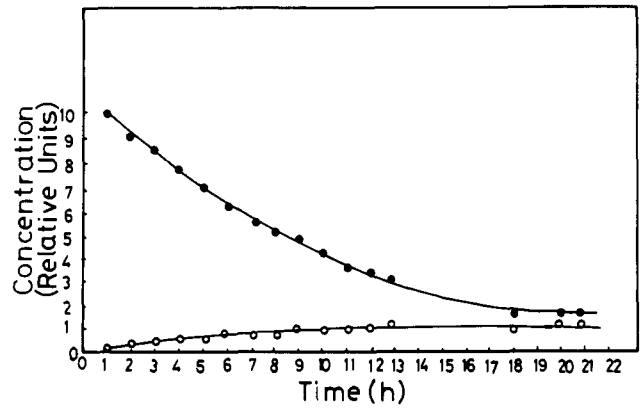

Figure 2. The plots of concentrations of dimer (●) and monomer (○) vs time after stirring as determined by ^1H NMR.

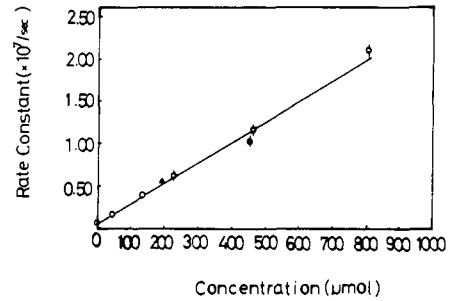

Figure 3. The plots of k_I vs concentration of the MNP dimer. The experiments were repeated 5–9 times. The error bars represent standard deviations.

concentration of the monomer increased slowly with time. Dimer–monomer equilibrium was reached after 18 h of bubbling. However, this figure indicates that the amount of decrease of the dimer was not necessarily reflected in the production of the monomer. The MNP dimer might decompose to compounds other than the monomer.[12] Figure 1c shows the NMR spectrum when the solution of Figure 1a was again bubbled with Ar gas for 30 min. The monomer was almost removed by bubbling, and the ratio of [dimer]/[monomer] markedly increased to 74.

Pulse radiolysis experiments were carried out to determine the reaction rate constant between e_{aq}^- and MNP. The nanosecond pulse radiolysis system used has been described in detail elsewhere.[13,14] An aqueous solution was bubbled with Ar gas and stored for appropriate times to get various concentrations of dimer and monomer as shown in Figure 2. The reaction rates, $k_I = k(e_{aq}^- + MNP) \times [MNP]$, were obtained from the decay curves at various concentrations of dimer or monomer. In Figure 3 the k_I's are plotted against the concentrations of the dimer. When the MNP solution of Figure 1b, where a 193 μM dimer and a 4.4 μM monomer were contained, was used, the k_I was found to lie nearly on the straight line (▲ in Figure 3). A similar observation was obtained for the MNP solution of Figure 1c, which contained a 450 μM dimer and a 6 μM monomer (● in Figure 3). These observations clearly indicate that the dominant form of MNP reacting with e_{aq}^- is the dimer. From Figure 3, the reaction rate constant (k) between e_{aq}^- and MNP was calculated to be $(2.4 \pm 0.1) \times 10^{10}$ mol^{-1} s^{-1} by linear regression analysis.

The present study has elucidated that although the active form of MNP trapping organic free radicals is the monomer,[3] e_{aq}^- reacts predominantly with the dimer. The present study will be helpful in minimizing the formation of byproducts in future spin trapping experiments with MNP. Similar experiments were carried out in N_2O-saturated aqueous solution containing MNP to determine reaction rate constants between MNP and OH• in the range of

(10) Sargent, F. P.; Gardy, E. M. *Can. J. Chem.* **1976**, *54*, 275–279.
(11) Greenstock, C. L. *Abstr. 61st Can. Chem. Congr.* **1978**, OR-5, 65.
(12) Makino, K.; Suzuki, N.; Moriya, F.; Rokushika, S.; Hatano, H. *Radiat. Res.* **1981**, *86*, 294–310.
(13) Kondo, T.; Aikawa, M.; Sumiyoshi, T.; Katayama, M. *J. Phys. Chem.* **1980**, *84*, 2544–2548.
(14) Maekawa, T.; Abe, M.; Yokokawa, T.; Sumiyoshi, T.; Sawamura, S.; Katayama, M. *Yogyo Kyokaishi* **1984**, *92*, 448–453.

wavelengths between 350 and 725 nm, but no transient species were observed in this wavelength range.[15]

Acknowledgment. We thank Dr. S. Shimokawa and Mr. M. Kitaichi, Faculty of Engineering, Hokkaido University, for the NMR and pulse radiolysis experiments.

Registry No. MNP, 917-95-3.

(15) Because of the strong light absorption due to the MNP dimer in the range of wavelengths between 200 and 350 nm, aqueous solutions containing low concentrations of MNP must be used for pulse radiolysis experiments at wavelengths below 350 nm. Nevertheless, an absorbance spectrum could be observed in the range of wavelengths between 250 and 300 nm with a maximum absorbance at the wavelength around 275 nm after electron pulse irradiation and was regarded as the OH-induced transients of the MNP dimer. No information concerning the OH-induced transients of the monomer was obtained because preparation of an N_2O-saturated solution containing only the monomer was impossible. When the competition method using CNS^- as a reference solute was carried out to determine the rate constants between MNP and OH radicals, it was observed that the MNP monomer reacted more rapidly with OH radicals than the MNP dimer did in the solution that both monomer and dimer coexisted, and the rate constant between the MNP monomer and OH radicals was roughly estimated to be 6×10^9 mol^{-1} s^{-1}.

Reevaluation of the Stereochemical Courses of the Allylic Rearrangement and the Double-Bond Reduction Catalyzed by *Brevibacterium ammoniagenes* Fatty Acid Synthase

Mary C. O'Sullivan and John M. Schwab*

Department of Medicinal Chemistry and Pharmacognosy
School of Pharmacy, Purdue University
West Lafayette, Indiana 47907

T. Mark Zabriskie, Gregory L. Helms, and John C. Vederas

Department of Chemistry, University of Alberta
Edmonton, Alberta, Canada T6G 2G2
Received November 14, 1990

Substrates for enzymatic allylic rearrangements[1] belong to two general groups: (a) those with isolated allylic systems and (b) those from which resonance-stabilized carbanions could in principle be formed (cf. **1**).[2] Studies of net reaction stereochemistry have revealed striking mechanistic uniformity among the allylic rearrangements of the second group:[1,3] With one reported exception,[4] all of these reactions proceed suprafacially, suggesting a single active site acid/base.[5,6]

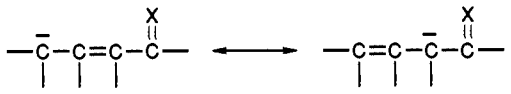

1

The exception is the fatty acid synthase (FAS) of *Brevibacterium ammoniagenes*, a multienzyme complex[7] producing both saturated and monounsaturated[8] fatty acids. The critical reaction in the O_2-independent pathway to unsaturated fatty acids in *B. ammoniagenes* is the allylic rearrangement of enzyme-bound (*E*)-2-dodecenoyl thiol ester **3** to (*Z*)-3-dodecenoyl thiol ester **4**. Compound **3** can be reduced and elongated to saturated fatty acids,

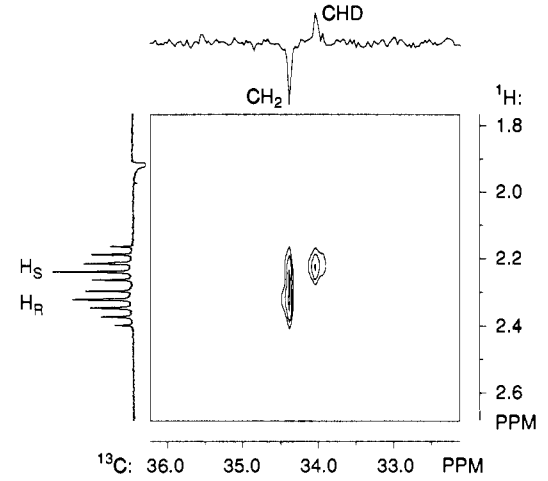

Figure 1. ^{2}H-decoupled HETCOR spectrum of the C-2 CH_2 group of **5** from the degradation of oleic acid derived from sodium [2-^{13}C,$^2H_3$]-acetate. The ^{13}C spectrum shown in the horizontal dimension was obtained by using a DEPT pulse sequence.

while direct elongation of **4** gives monounsaturated fatty acids including oleic (9-octadecenoic) acid.

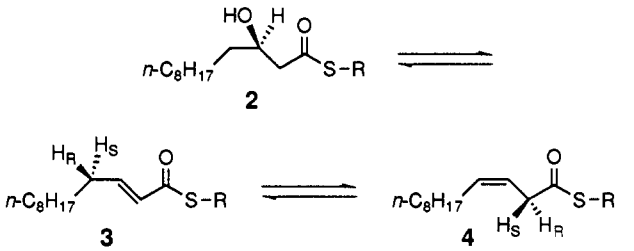

It has been suggested that the *B. ammoniagenes* FAS interconverts **3** and **4** via an antarafacial rearrangement.[4] We now show that this process is suprafacial and that the overall steric course of the enoyl reductase step of fatty acid biosynthesis by the *B. ammoniagenes* FAS is anti, rather than syn as proposed previously.[9]

Following the strategy of Vederas and co-workers,[10-16] *B. ammoniagenes* was grown on sodium [2-^{13}C,$^2H_3$]acetate, and methyl oleate was isolated.[17] The ^{1}H-decoupled ^{2}H NMR spectrum of

(1) Schwab, J. M.; Henderson, B. S. *Chem. Rev.* **1990**, *90*, 1203–1245.
(2) This is not meant to imply that such carbanions are necessarily the enzymatic reaction intermediates.
(3) Schwab, J. M.; Klassen, J. B. *J. Am. Chem. Soc.* **1984**, *106*, 7217–7227.
(4) Saito, K.; Kawaguchi, A.; Seyama, Y.; Yamakawa, T.; Okuda, S. *Tetrahedron Lett.* **1982**, *23*, 1689–1692.
(5) Hanson, K. R.; Rose, I. A. *Acc. Chem. Res.* **1975**, *8*, 1–10.
(6) Rose, I. A.; Hanson, K. R. In *Applications of Biochemical Systems in Organic Chemistry*; Jones, J. B., Sih, C. J., Perlman, D., Eds.; Wiley: Oxford, 1976; Vol. 10, Part 2; pp 507–553.
(7) Morishima, N.; Ikai, A.; Noda, H.; Kawaguchi, A. *Biochim. Biophys. Acta* **1982**, *708*, 305–312.
(8) Kawaguchi, A.; Okuda, S. *Proc. Natl. Acad. Sci. U.S.A.* **1977**, *74*, 3180–3183.
(9) Saito, K.; Kawaguchi, A.; Seyama, Y.; Yamakawa, T.; Okuda, S. *J. Biochem.* **1981**, *90*, 1697–1704.
(10) Trimble, L. A.; Reese, P. B.; Vederas, J. C. *J. Am. Chem. Soc.* **1985**, *107*, 2175–2177.
(11) Reese, P. B.; Trimble, L. A.; Vederas, J. C. *Can. J. Chem.* **1986**, *64*, 1427–1434.
(12) Reese, P. B.; Rawlings, B. J.; Ramer, S. E.; Vederas, J. C. *J. Am. Chem. Soc.* **1988**, *110*, 316–318.
(13) Townsend, C. A.; Brobst, S. W.; Ramer, S. E.; Vederas, J. C. *J. Am. Chem. Soc.* **1988**, *110*, 318–319.
(14) Rawlings, B. J.; Reese, P. B.; Ramer, S. E.; Vederas, J. C. *J. Am. Chem. Soc.* **1989**, *111*, 3382–3390.
(15) Arai, K.; Rawlings, B. J.; Yoshizawa, Y.; Vederas, J. C. *J. Am. Chem. Soc.* **1989**, *111*, 3391–3399.
(16) Oikawa, H.; Yokota, T.; Abe, T.; Ichihara, A.; Sakamura, S.; Yoshizawa, Y.; Vederas, J. C. *J. Chem. Soc., Chem. Commun.* **1989**, 1282–1284.
(17) Nutrient broth (2 L) containing sodium [2-^{13}C,$^2H_3$]acetate (1 g) and unlabeled sodium acetate (1 g) was inoculated with *B. ammoniagenes* ATCC 6871 (the strain used by Kawaguchi and co-workers for studies of *B. ammoniagenes* FAS[8]) and incubated at 30 °C with shaking (220 rpm) for 27 h. The cells were collected by centrifugation and resuspended along with silica gel (230–400 mesh; 50 g) in deionized water (100 mL). The mixture was homogenized in a Waring blender for 20 min, 1:1 $CHCl_3$/MeOH (600 mL) added, and the mixture stirred overnight. The suspension was filtered and the crude fatty acid extract saponified with potassium *tert*-butoxide (3.0 g) and water (0.486 mL) in tetrahydrofuran (70 mL) at room temperature overnight. The solvent was removed, 5% HCl was added, and the aqueous phase was extracted with CH_2Cl_2. The residue from removal of the solvent was purified by flash chromatography (2–4%, MeOH in CH_2Cl_2) to give a mixture of fatty acids (48 mg), which was treated with excess ethereal CH_2N_2 to give a mixture of fatty acid methyl esters (54 mg). Preparative TLC in the dark (silica gel impregnated with 20% $AgNO_3$ (Analtech); 1% MeOH in CH_2Cl_2) gave methyl oleate (34 mg) and a mixture of methyl esters of saturated fatty acids.

0002-7863/91/1513-3997$02.50/0